ENGINEERING RESEARCH JOURNAL (ERJ)

Vol. 1, No. 41 July. 2019, pp. 1-8

Journal Homepage: www.feng.bu.edu.eg

Effect of Process Parameters on Microstructure and Mechanical Properties of Aluminum Alloy AA2024-T6 Friction Stir Spot Welded Joints

A. M. Gaafer

Mechanical Engineering Department, Faculty of Engineering, Benha University, 108 Shoubra st., Cairo, Egypt

Abstract. In the presented paper the friction stir spot welding process is performed on AA2024-T6. The welding was carried out on a CNC milling machine at different rotational speeds of 1500, 2000 and 2500 rpm, and different plunge depths of 1, 1.25 and 1.5 mm. The welded joints were examined by SEM and the percentage of precipitates was measured by EDS. The joints were tested mechanically for hardness and tension shear. The highest grains size and tensile shear load was obtained at 2500 rpm and 1.5 mm; while the highest average hardness value was obtained at 2000 rpm and 1.5 mm.

Keywords: Friction Stir spot welding, AA2024-T6, SEM, Mechanical properties

1. INTRODUCTION

Friction stir spot welding (FSSW) is a thermo-mechanical process for spot lap-joining of sheet metals [**1**]. In FSSW a non-consumable rotating tool is used to generate frictional heating and produce plasticized region at the bonding interface as a result of a strong compressive forging pressure. The cross section of the spot weld is divided into four zones as follows: Base Material (BM), Heat Affected Zone (HAZ), Thermo-mechanically Affected Zone (TMAZ) and Stir Zone (SZ) [**2**].

As a relatively new manufacturing process, there is very limited published research on FSSW process. Zhang et al. [**3**] studied the effect of welding parameters on microstructural and mechanical properties of AA5052 friction stir spot welded joints. Uematsu et al. [**4**] joined AA6061-T4 by using a double acting tool consisting of outer flat shoulder and inner retractable probe, which could re-fill probe hole. Merzoug et al. [**5**] conducted experiments on AA6060-T5 by using a tool steel of the type X210 CR 12 and the rotational speed of the tool ranged from 1000 to 2000 rpm. Shen et al. [**6**] studied the effect of rotational speed and dwell time on AA 7075-T6 friction stir spot welded joints. Tozaki et al [**7**] investigated the effect of tool pin length on AA6061-T4 welded joints. Badarinarayan et al. [**8**] joined AA 5083-O sheets by using tool with a concave shoulder of 12 mm diameter. Suhddin et al. [**9**] have performed the FSSW process on AA5754 and Mg alloy AZ31. They reported on the effect of the process parameters on the thermal cycle, microstructural and mechanical properties of the welded joints. Heideman et al. [**10**] have investigated the effect of FSSW parameters on the material characterization of dissimilar aluminum-copper welded joints. Piccini et al. [**11**] have studied the effect of tool pin length on the microstructural and the mechanical properties of dissimilar aluminum- galvanized steel friction stir spot welded joints. Sun et al. [**12**] welded AA6061 with mild steel by using FSSW technique and studied the microstructural evolution the mechanical properties of the welded joints. Therefore, the aim of this research is to study the effect of FSSW parameters on AA2024-T6 joints.

2. Experimental Investigation

2.1 FSSW process and operation conditions

Aluminum alloy AA 2024-T6 plates of dimensions 175 mm x 50 mm x 3.5 mm were friction stir spot welded on a CNC milling machine by using H13 tool steel whose schematic drawing shown in **Fig. 1**. The chemical composition and the mechanical properties of AA2024-T6 are shown in **tables 1** and **2** respectively; while the welding process parameters are summarized in **table 3**.

2.2 Material characterization

The surfaces of all specimens were grinded, polished and etched using Keller etching reagent [190 ml H_2O, 3 ml HNO_3, 2 ml HF, and 3mL HCl] of period 1.5-2 minutes and the microstructure evolutions were examined by using an Olympus optical PMG3 microscope. The chemical composition of the elements and second phases was analyzed by a scanning electron microscope (SEM) equipped with energy dispersive X- ray spectroscopy (EDS) using stereoscope Nikon SMZ-10.

2.3 Mechanical testing

The mechanical properties, mainly tensile strength and hardness, were measured for each sample.

2.3.1 Tensile-Shear Test

Tensile-shear tests were carried out to evaluate the performance of the welds. Lap-shear specimens according to DIN EN-ISO 14273 standard as shown in **Fig. 2**. Tensile-shear tests were carried out by using a universal testing machine and the average of three specimens was calculated for each welded joint.

2.3.2 Microhardness test

Vickers micro hardness profile is measured on the traverse section along a plane 0.5 mm under the shoulder plunge face of the two overlapped sheets using an indenting load of 10 Kg at loading time of 15 seconds.

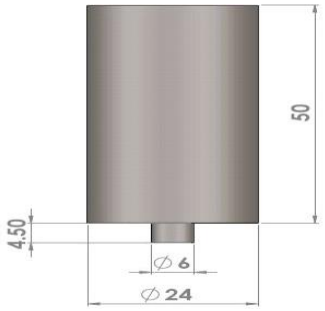

Fig. 1 Schematic drawing of FSSW tool

Table 1 The chemical composition of AA2024

Al	Cr	Cu	Fe	Mg	Mn	Si	Ti	Zn	Other
94.90	0.01	4.30	-	0.10	0.35	0.08	0.06	0.011	0.189

Table 1 The chemical composition of AA2024

Tensile strength [MPa]	Yield strength [MPa]	Vickers Hardness [HV]
427	345	142

Table 3 FSSW operation conditions

Rotational speed (rpm)	Plunge depth (mm)	Dwell time (Sec.)
1500, 2000, 2500	1, 1.25, 1.5	10

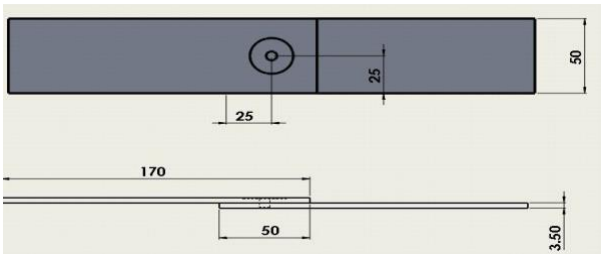

Fig. 2 Lap tensile shear test specimen

3. Results and Discussion

3.1 Effect of FSSW process parameters on the microstructure evolutions of the welded joints

3.1.1 Optical micrograph and SEM Examinations of the welded joints

Typical microstructures of the SZ observed for the welded joints at different rotational and plunge depth values as shown in **Fig. 3**; while the SEM examination are presented in **Fig. 4**. As can be seen from both figures, the stir zones exhibited very fine recrystallized equiaxed grains and the grains sizes increase with increasing rotational speed values. F**ig. 5** plots the grains sizes variation due to variation of both rotational speed and plunge depth values. As can be observed from the graph shown, the grains sizes increase with increasing both rotational speed and plunge depth values. It is worth noting that the highest grains sizes are obtained at higher rotational speed and plunge depth values. This coarsening and growth of the grains may be attributed to the higher heat input generated from higher rotational speed as mentioned by El-Sayed et al. [13].

3.1.2 SEM-EDS analysis of the

The SEM-EDS analysis is used to detect the types of inclusions in welded joints. The SEM-EDS maps analyses for Al, Cu, Mg, Fe, Ti and Mn for the SZ at 1500 rpm and 1.25 mm are shown in **Fig. 6.** The figure shows regions contain high concentrations of various elements like; Cu, Fe, Mn and Ti. Some of these regions/phases were spot analyzed by using EDS spot analysis yielding the results presented in **Fig. 7**. The analysis of region (**a**) in **Fig. 6** is shown in **Fig. 7** (point **X**) which represents analyses of $CuAl_2$ inclusions in this phase. On the other hand the analysis of region (**b**) in **Fig. 8** is represented in **Fig. 9 (**point **Y)** which indicates that the inclusions containing Al– Cu–Fe–Si–Mn particles and $CuAl_2$ phase which resulted in strengthening the alloy through a precipitationstrengthening mechanism, which involves obstructing movement of dislocations due the presence of the secondphase particles in the alloy.

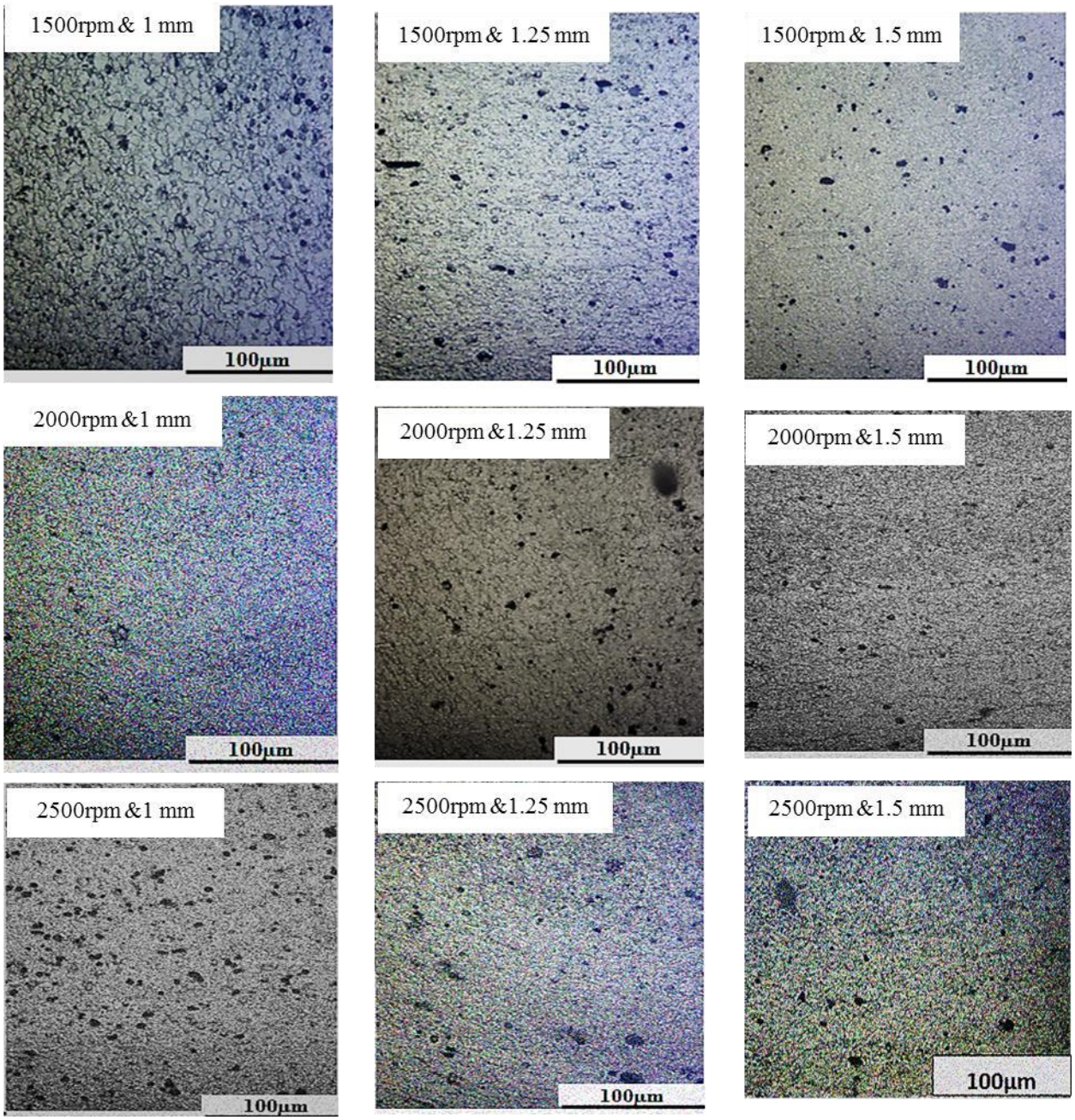

Fig. 3 Optical micrograph of the welded joints at different rotational speed and plunge depth values

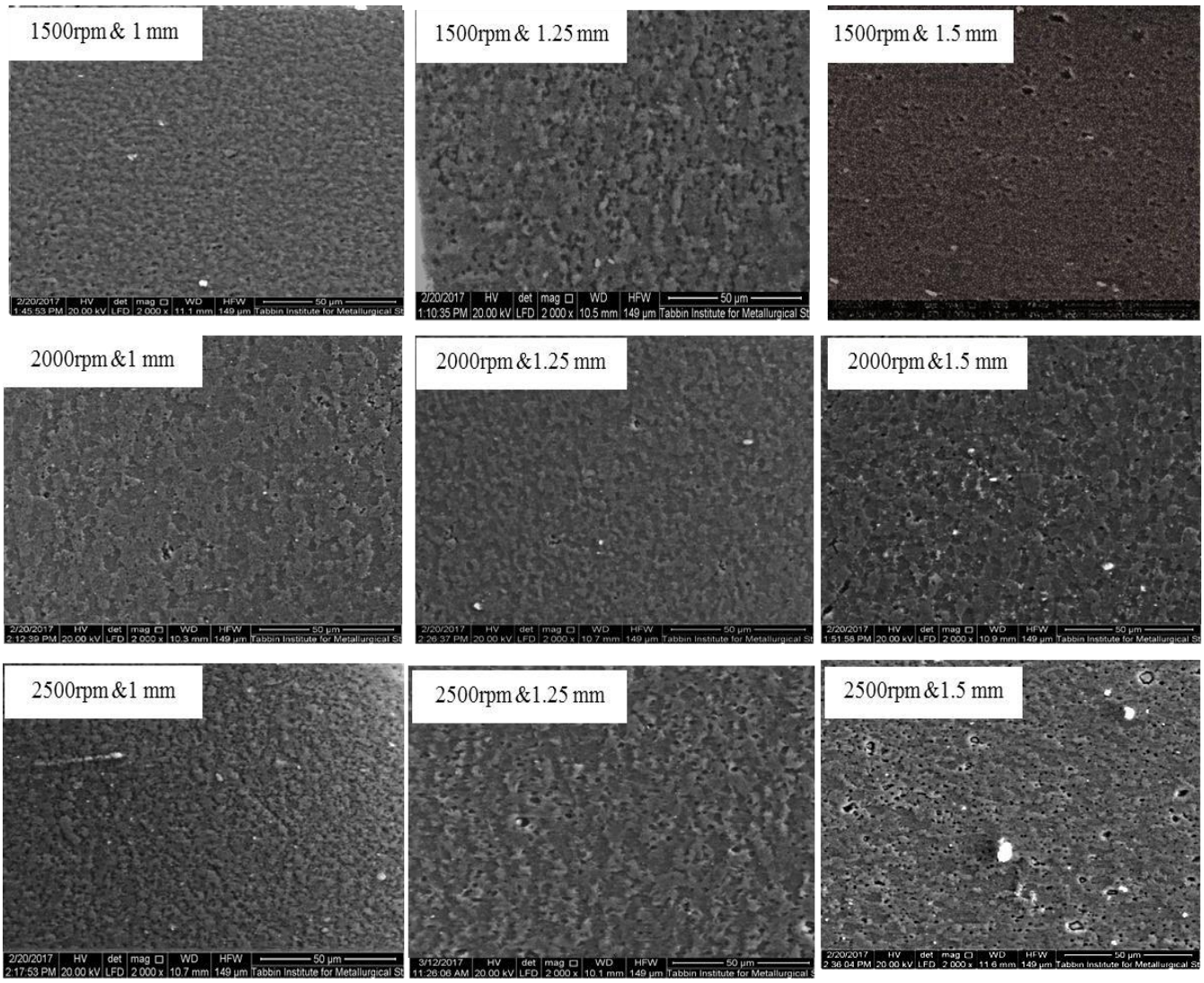

Fig. 4 SEM microstructure the SZ at different rotational speed and plunge depth values

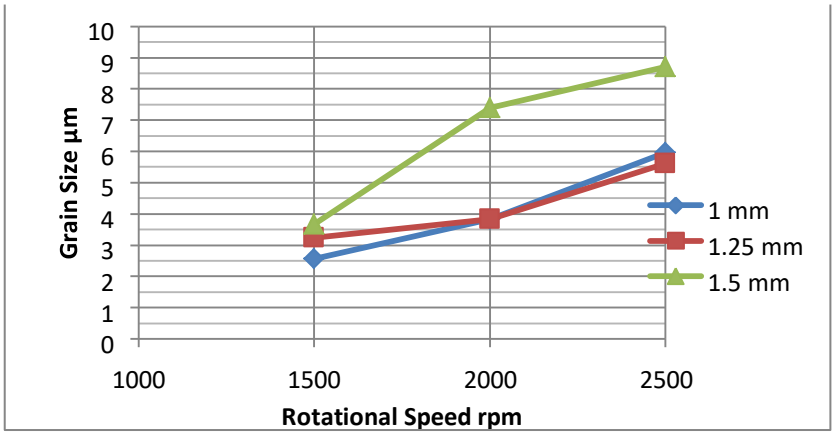

Fig. 5 Grains sizes variation due to variation of rotational speed and plunge depth values

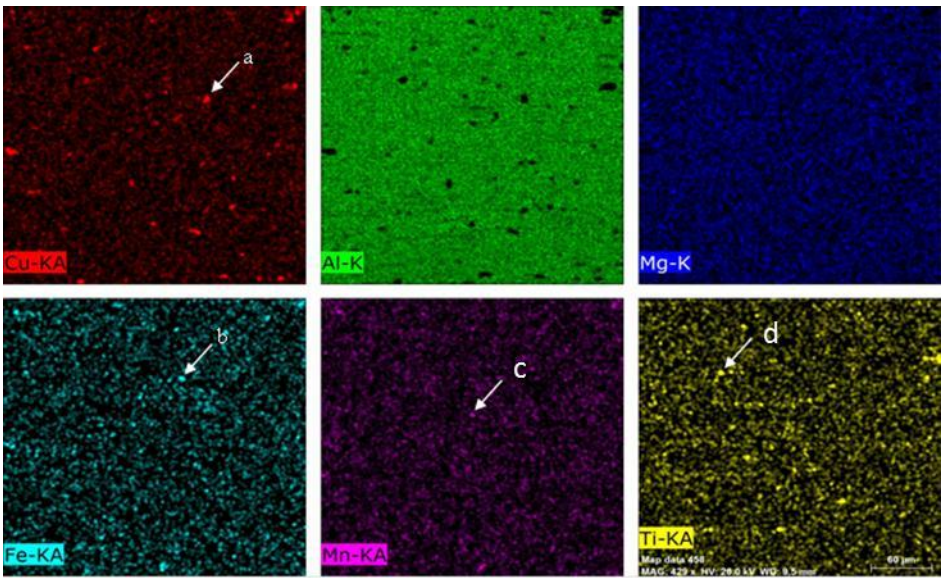

Fig. 6 SEM-EDS map analysis of the SZ at 1500 rpm & 1.25 mm

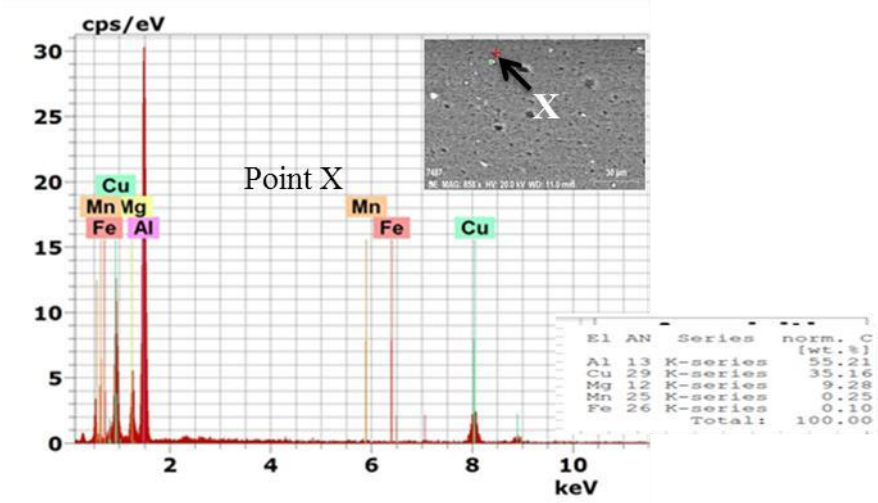

Fig. 7 SEM-EDS spot analysis of the SZ at 1500 rpm & 1.25 mm

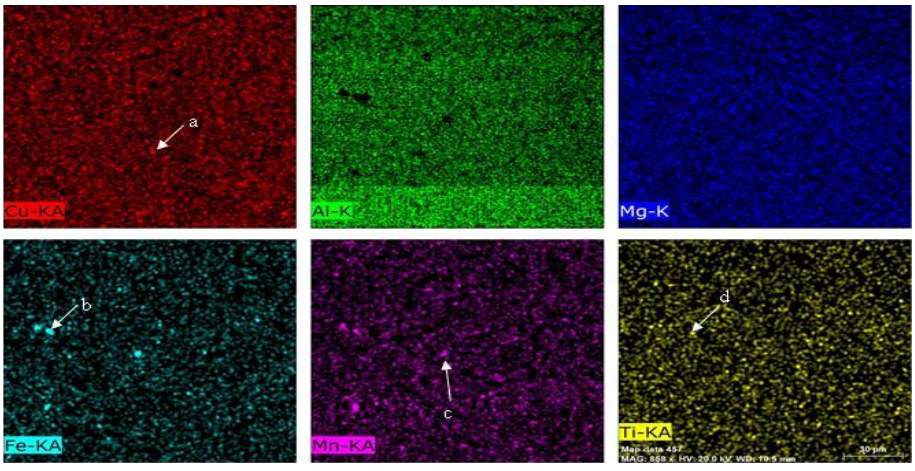

Fig. 8 SEM-EDS map analysis of the SZ at 2000 rpm & 1.5 mm

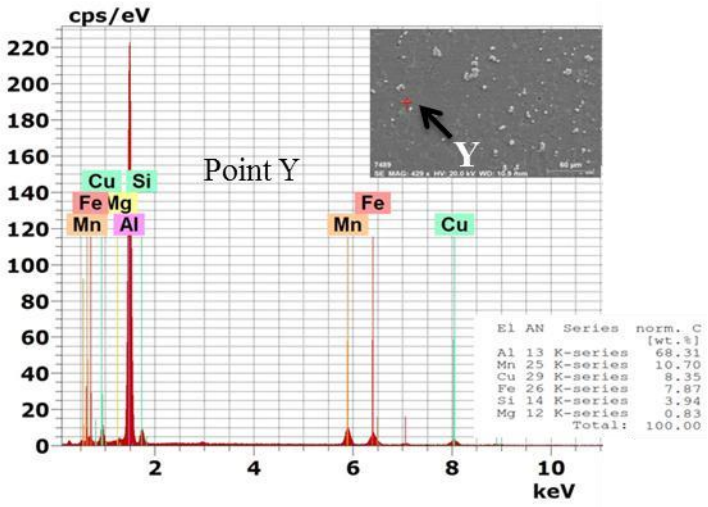

Fig. 9 SEM-EDS spot analysis of the SZ at 2000 rpm & 1.5 mm

1.1 Effect of FSSW process parameters on the mechanical properties of the welded joints

Figure 10 shows typical micro hardness profiles of the welded joints. The results revealed that the welds have a higher micro hardness in the stir zone than other zones. The micro hardness increases toward the direction of the pinhole. The hardness was found to be no symmetric with respect to center of the pinhole. It also noticeable that almost welding conditions have hardness values higher than base material (BM) at the SZ.

Regarding **Fig. 11** which depicts the effect of rotational speed and plunge depth on the average hardness values in the SZ. As obviously noticed in this figure, the average hardness values fluctuate with variation of rotational speeds at 1 mm and 1.25 mm plunge depth values; while these values increase with increasing rotational speed at 1.5 mm. It is worth noting that the average hardness values at 2500 rpm are observed to be lower than those obtained at other rotational speeds at 1 mm and 1.25 mm because of the higher grains sizes in the SZ resulted from their growth and coarsening.

On the other hand **Fig. 12** represents the variation of tensile shear load due to variation of both rotational speed and plunge depth values. It is observed from the demonstrated figure, the tensile shear load values increase due to increasing rotational speed values at 1 mm and 1.5 mm plunge depth values; whereas these values fluctuate with changing rotational speeds at 1.25 mm plunge depth. It is noticeable that the highest tensile strength value obtained at 2500 rpm rotational speed and 1.5 mm plunge depth.

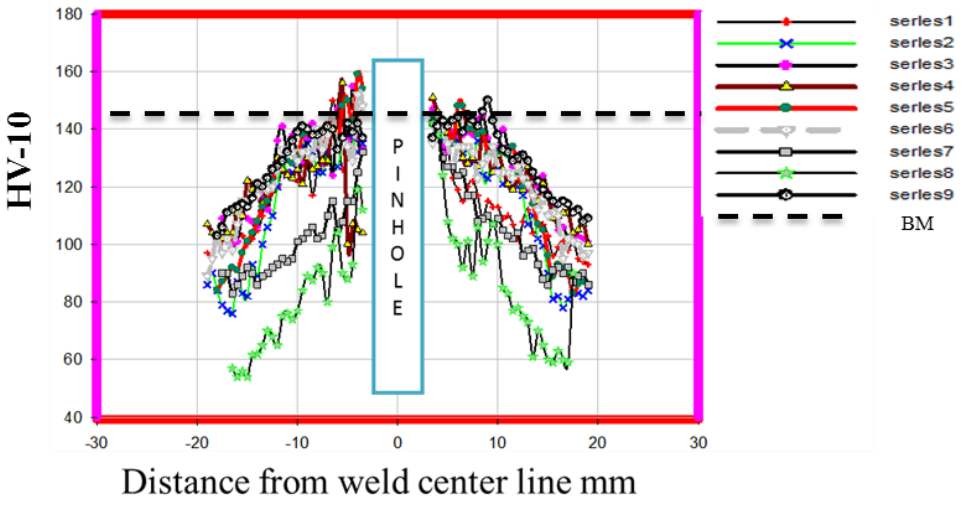

Fig. 10 Vickers Microhardness profiles at different rotational and plunge depth values

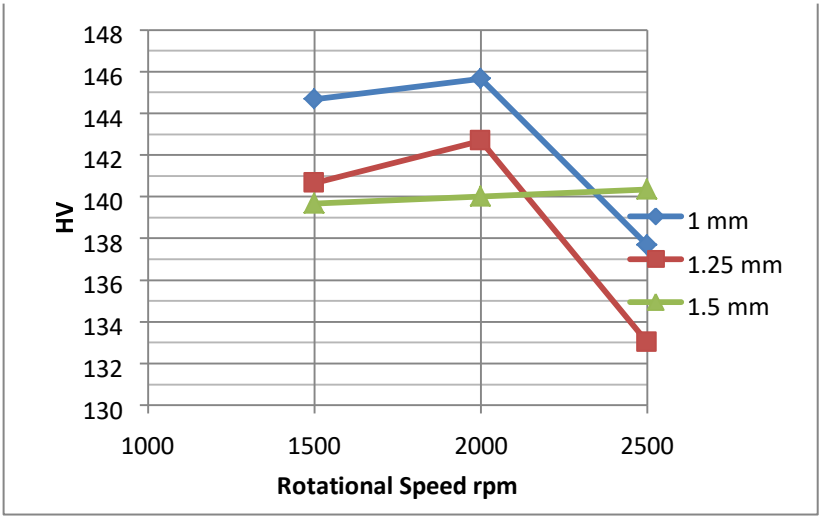

Fig. 11 Average hardness variation due to variation of rotational speed and plunge depth values

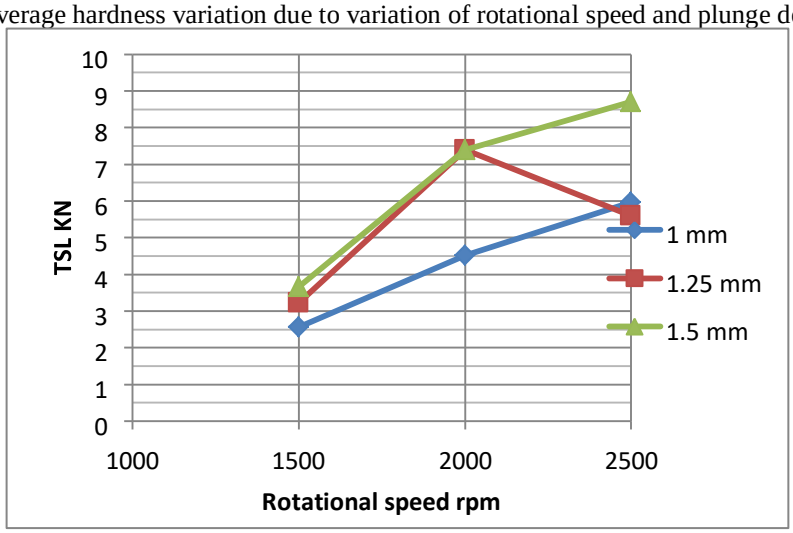

Fig. 12 Tensile shear load variation due to variation of rotational speed and plunge depth values

2. Conclusions

From the examinations that have been conducted, it is possible to conclude that

1- The plunge depth approximately has no effect on the grains size at lower rotational speed (i.e. 1500 & 2000 rpm); while it has a great effect at higher rotational speed (i.e. 2500 rpm).

2- The variation of plunge depth has an effect on the average hardness values in the SZ at all rotational speed values.

3- The highest hardness value was obtained at 2000 rpm and 1 mm; while the lowest one was obtained at 2500 rpm and 1.25 mm.

4- The variation of rotational speed has a great effect on the tensile shear load at plunge depth values.

5- The plunge depth approximately has no effect on the tensile shear load at 1500 rpm; while it has an effect at other rotational speed values.

6- The maximum tensile shear load was obtained at 2500 rpm and 1.5 mm; while the lowest one was obtained at 1500 rpm and 1 mm.

References

[1] Rao H. M., Jordon J. B., Barkey M. E., Guo Y. B., Su X., Badarinarayan H. Influence of structural integrity on fatigue behavior of friction stir spot welded AZ31 Mg alloy. Materials Science & Engineering A. 2013; 564: 369380.

[2] Badarinarayan H. Fundamentals of friction stir spot welding. PhD thesis, Missouri University of Science and Technology, United State' 2009.

[3] Zhang Z., Yang X., Zhang J., Zhou G., Xu X., Zou B. Effect of welding parameters on microstructure and mechanical properties of friction stir spot welded 5052 aluminium alloy. Materials and Design 2011; 32: 4461– 4470.

[4] Uematsu Y., Tokaji K., Tozaki Y., Kurita T., Murata S. Effect of refilling probe hole on tensile failure and fatigue behaviour of friction stir spot welded joints in Al–Mg–Si alloy. International Journal of Fatigue 2008; 30: 1956–1966.

[5] Timothy J M., 'Friction Stir Welding of Commercially available Superplastic Aluminium. PhD thesis, Department of Engineering and Design, Brunel University, Brunel, 2008.

[6] Zhikang Shen, Xinqi Yang, Zhaohua Zhang, Lei Cui, Tielong Li. Microstructure and failure mechanisms of refill friction stir spot welded 7075-T6 aluminium alloy joints. Materials and Design 2013; 44:476–486.

[7] Yasunari Tozaki, Yoshihiko Uematsu , Keiro Tokaji. Effect of tool geometry on microstructure and static strength in friction stir spot welded aluminium alloys. International Journal of Machine Tools & Manufacture 2007; 447: 2230–2236.

[8] Badarinarayan, H., Q. Yang, and S. Zhu. Effect of tool geometry on static strength of friction stir spot-welded aluminium alloy. International Journal of Machine Tools and Manufacture 2009; 49: 142-148.

[9] Suhuddin U.F.H., Fischer V. and dos Santos J.F. The thermal cycle during the dissimilar friction spot welding of aluminum and magnesium alloy. Scripta Materialia 2013; 68: 87–90.

[10] Heideman R., Johnson C., Kou S., Metallurgical analysis of Al/Cu friction stir spot welding. Science and Technology of Welding and Joining 2010; 15: 597-604.

[11] Piccinia J. M., Svoboda H. G. Effect of pin length on Friction Stir Spot Welding (FSSW) of dissimilar Aluminum-Steel joints. Procedia Materials Science 2015; 9: 504 – 513.

[12] Sun Y.F., Fujii H., Takaki N., Okitsu Y. Microstructure and mechanical properties of dissimilar Al alloy/steel joints prepared by a flat spot friction stir welding technique. Materials and Design 2013; 47: 350–357.

[13] El-Sayed M.M., Shash A. Y. and Abd-Rabou M. Finite element modeling of aluminum alloy AA5083-O friction stir welding process. Jrnal of materials processing technology 2018; 252: 13-24.